A Report Submitted to
the National Aeronautics and Space Administration
Planetary Atmospheres Program
for Grant NASW-1908
Entitled:

Analysis of CCD Images of the Coma of Comet P/Halley

by Michael R. Combi

Space Physics Research Laboratory
Department of Atmospheric, Oceanic and Space Sciences
University of Michigan
Ann Arbor, MI 48109

December 1992

I. Introduction

The apparition of comet P/Halley during 1985 and 1986 permitted extensive observations of all types to be made. One important technique which was available only shortly before this apparition was the ability to obtain CCD images of the coma using various filters. This project deals with the analysis of selected CCD images of the coma of comet P/Halley which were taken using specially designed filters that isolate regions of a comet's spectrum such that only sunlight which has been scattered by the dust in the coma is recorded. The data addressed here are subsets of two larger datasets which also contain images taken with filters designed to pass regions of the spectrum which in addition to dust continuum include the spectral emissions of certain gas species and spectra. One of the sets of CCD images were taken with the 61-inch Wyeth telescope at the Oak Ridge Observatory by Dr. R.E. McCrosky of the Center for Astrophysics/Smithsonian Astrophysical Observatory. The second set of data were taken with the 61-inch telescope on Mt. Lemmon by Dr. Uwe Fink and co-workers at the Lunar and Planetary Laboratory of the University of Arizona. Since the object of project is the study of the dust distribution as evidenced in so-called "continuum" images the second complementary set of data were linear cut spatial profiles of dust extracted from long-slit CCD spectrograms of comet Halley.

The modeling analysis objective of this project is to make use of the skills acquired in the development of Monte Carlo particle trajectory models for the distributions of gas species in cometary comae (Combi and Smyth 1988 a&b) as a basis for a new dust coma model. This model will includes a self-consistent picture of the time-dependent dusty-gas dynamics of the inner coma and the three-dimensional time-dependent trajectories of the dust particles under the influence of solar gravity and solar radiation pressure in the outer coma. Our purpose is to use this model as a tool to analyze selected images from the two sets of data with the hope that we can help to understand the effects of a number of important processes on the spatial morphology of the observed dust coma. The study will proceed much in the same way as our study of the spatially extended hydrogen coma (Combi and Smyth 1988b) where we were able to understand the spatial morphology of the Lyman-alpha coma in terms of the partial thermalization of the hot H atoms produced by the photodissociation of cometary H_2O and OH.

The processes of importance to the observed dust coma include:

(1) the dust particle size distribution function,

(2) the terminal velocities of various sized dust particles in the inner coma,

(3) the radiation scattering properties of dust particles, which are important both in terms of the observed scattered radiation and the radiation pressure acceleration on dust particles,
(4) the fragmentation and/or vaporization of dust particles, and
(5) the relative importance of CHON and silicate dust particles as they contribute both to the dusty-gasdynamics in the inner coma (that produce the dust particle terminal velocities) and to the observed spatial morphology of the outer dust coma.
(6) the time and direction dependence of the source of dust.

In work completed to this point in time we have made substantial progress in addressing directly points 1-4 and 6 At this time we find ourselves just short of describing our results in two papers: one describing the dust model and application to dust coma images, and a second using that model to study time-variable sunward and antisunward spatial profiles of dust in comet Halley. Preliminary results, summarizing both aspects of the work were presented at the 1992 meeting of the Division for Planetary Sciences held in Munich, Germany (Combi and Fink 1992). A copy of the talk is attached as an appendix to this report. This work is to continue as part of a new 3-year effort which has been tentatively approved by the Planetary Atmospheres program.

II. Development of the Dust Model

The basic framework of the dust model lay in the core of the hydrogen coma model discussed in detail in the papers by Combi and Smyth (1988 a& b). It is a fully 3-D time-dependent Monte Carlo particle trajectory model that builds up an entire coma by tracing out the trajectories of many individual particles. For the published gas coma model the particles are individual atoms, radicals and molecules; for the dust model the particles are obviously individual dust particles. Recently Jewitt and Luu (1990) have published the results of a Monte Carlo dust coma model applied to observations of Comet P/Tempel 2. However, their model is steady-state, and spherical. Ellis and Neff (1991) have recently developed a numerical dust model for neutral or charged dust for comparison with dust experiments on Vega 1 and 2 and Giotto. However, their results state that the dust particle terminal velocities required to match their model to data are 1.7 times the values implied by conventionally dusty gasdynamics. Unfortunately, the resulting dust velocities would exceed the velocity of the gas that is accelerating the dust! Clearly this is not possible.

The standard dust coma treatment goes back to the pioneering work of Finson and Probstein (1968) which considers the dust to consist of a population of particles having a variation of sizes with a size distribution determined by some power law in particle diameter. The particles are considered to have a constant density, $\rho(a) = \rho_o$, independent of particle size,. The light scattering properties which are needed not only to describe the observed scattered radiation but also to calculate the radiation pressure acceleration on each particle size are considered to be simply proportional to the geometric cross section of the particle. The latter two conditions implying that the light scattering efficiency, Q_{scat}, and the radiation pressure efficiency, η_{rp}, both equal unity.

From polarization measurements of Comet Halley (Mukai, et al., 1987) it is clear that cometary grains at least share the optical properties of a material called astronomical silicate. Hoban, et al. (1989) have analyzed dust images of comet Halley in this context, however not with a detailed coma model like is that under development for this project. Although we certainly expect that many real cometary grains are not spherical but may be quite irregular, the adoption of Mie theory which assumes spherical particles has proven to be quite useful by other investigators. Figure 1 shows a plot of the results of Mie calculations by Hoban et al. which we have adopted for the light scattering properties in our model.

In Figure 2 are shown the results of Hellmich and Schwehm (1983) for the radiation pressure efficiency as a function of size for dark dielectric material which is believed to be indicative of cometary dust particle. Notice that the radiation pressure efficiency drops precipitously for very small particles and peaks for particles who sizes are in the range of the wavelength of the peak of the solar radiation. We have adopted this as the standard radiation pressure efficiency.

Therefore, for this work we have begun by adopting the optical properties of dark absorbing spheres. Probably the most uncertain aspect of this problem is not the optical properties of the dust grains but their densities. Although it has been traditional to assume densities of 1 to 3 g cm^{-3} it is likely that cometary grains are porous aggregates and therefore have a density which decreases with increasing radius. Lamy et al. (1987) have suggested a dust density of the form

$$\rho(a) = 2.2 - 1.4\, a/(a_0 - a).$$

where a = particle radius and a_o = 2 microns. We have chosen this as a starting point for our studies.

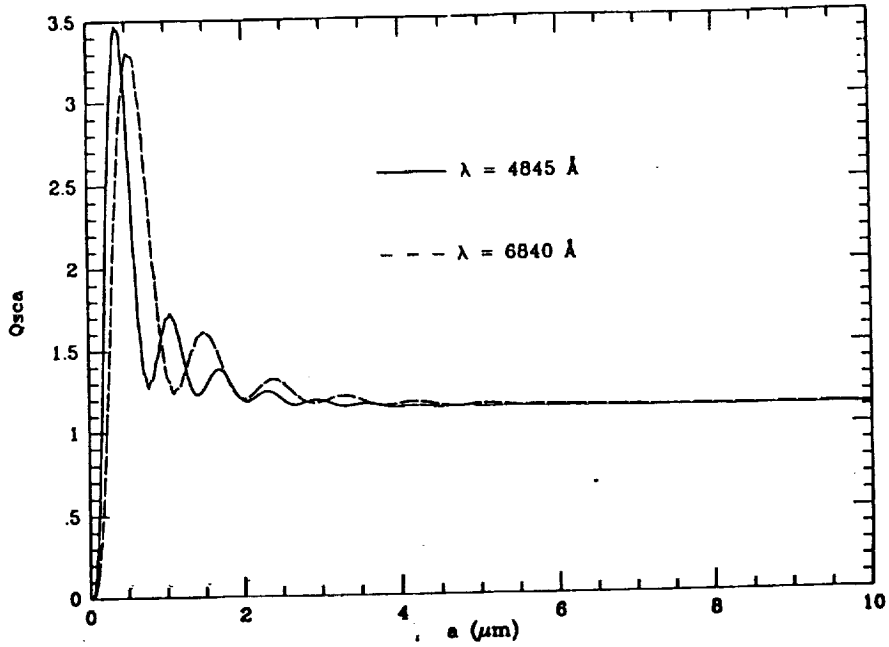

Figure 1. Single Particle Mie Scattering Efficiency as a Function of Particle Radius. The values of Qscat as calculated by Hoban et al. (1989) for the two IAU continuum filters are plotted. These calculations have been adopted in out dust coma model.

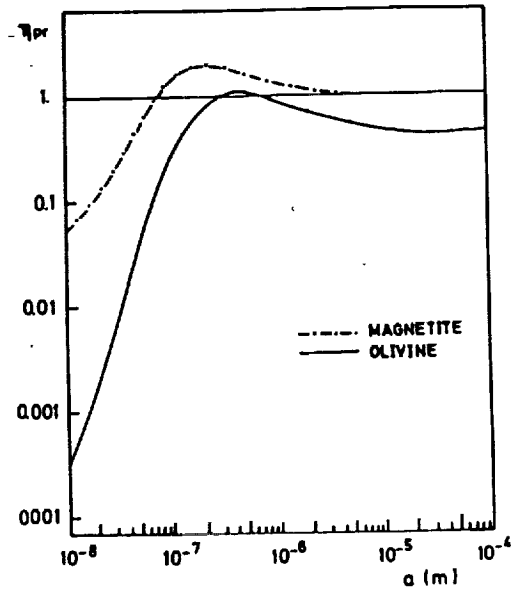

Figure 2. Radiation Pressure Efficiency, η_{pr}, for Prospective Cometary Grains. The values of η_{pr} calculated by Hellmich and Schwehm (1983) are shown for nonabsorbing (olivine) and absorbing (magnetite) grains. We have adopted the curve for the absorbing magnetite grains in our model.

Probstein (1968) lay the groundwork for all subsequent treatments of dusty gasdynamics in terms of his model that is included in full hydrodynamic calculations (Wallis 1982; Marconi and Mendis 1983; Gombosi et al. 1986). An empirical method outlined in papers by Sekanina (1981) and Sekanina and Larson (1984) approximates the results of a full hydrodynamic calculation in a simple parametrized form which gives the dust particle terminal velocity given the dust-to-gas mass ratio, the gas production rate and the particle size and mass. It provides an excellent approximation to the results produced by the full hydrodynamics. We have verified this by reproducing the results of the Halley dust distribution in the paper by Gombosi (1986).

The global dust model proceeds by picking a certain number of dust particles to run in the whole simulation. Twenty-eight dust particle sizes whose radii are distributed logarithmically, following those of Gombosi (1986). The distribution of dust particles of a given size are taken from the Hanner-type distribution. For Halley Gombosi (1986) gives the values of the appropriate parameters in the expression which best describes the *in situ* data. The scattered radiation which contributes to the observed brightness is calculated from the Qscat in Figure 1, the dust particle cross section, $4\pi a^2$, and the abundance weight from the Hanner expression. Following Hoban et al. the model routinely generate maps at wavelengths corresponding to the two IAU continuum filters at 4845 Å and 6840 Å. Figure 5, which will be discussed in the next section of this report in more detail, shows an example of the 2-D coma map produced by the model.

Individual trajectories can be weighted according to a prescribed time dependence, either the long term secular heliocentric distance variation, or more interesting the short time periodic variations which have been observed in comets Halley and more recently in comet Levy that indicate the effect of the illumination of active areas as the nucleus rotates. For the secular variation of comet Halley we have adopted the power laws found by Schleicher (1991 private communication) of $r^{-2.3}$ for pre-perihelion and $r^{-1.9}$ for post-perihelion realizing that these may ultimately have to be adjusted to account for heliocentric distance variation in the overall dust terminal velocities. Individual trajectories can also be included (or not included) in order to produce images of dust comae produced from restricted areas on the nucleus such as sunward-hemisphere emission, for example. Subsequent sections of this report will illustrate this capability also.

III. Dust Coma Observations

Two examples of dust coma images taken by Dr. R.E. McCrosky are shown in Figures 3 and 4. Figure 1 shows the dust coma of comet P/Halley taken with the IAU filter at 4840 Å. Figure 2 shows the dust coma of comet P/Halley taken with the IAU filter at 6840 Å. One possible problem with the 4840 Å IAU filter suggested by Hoban et al. (1989) is that the wavelength range covered includes not just continuum but is contaminated by a small amount C_2 (1-0) emission. However, comparison of these two images shows only minor differences which can not be accounted for by the addition of C_2 emission to the 4840 Å image.

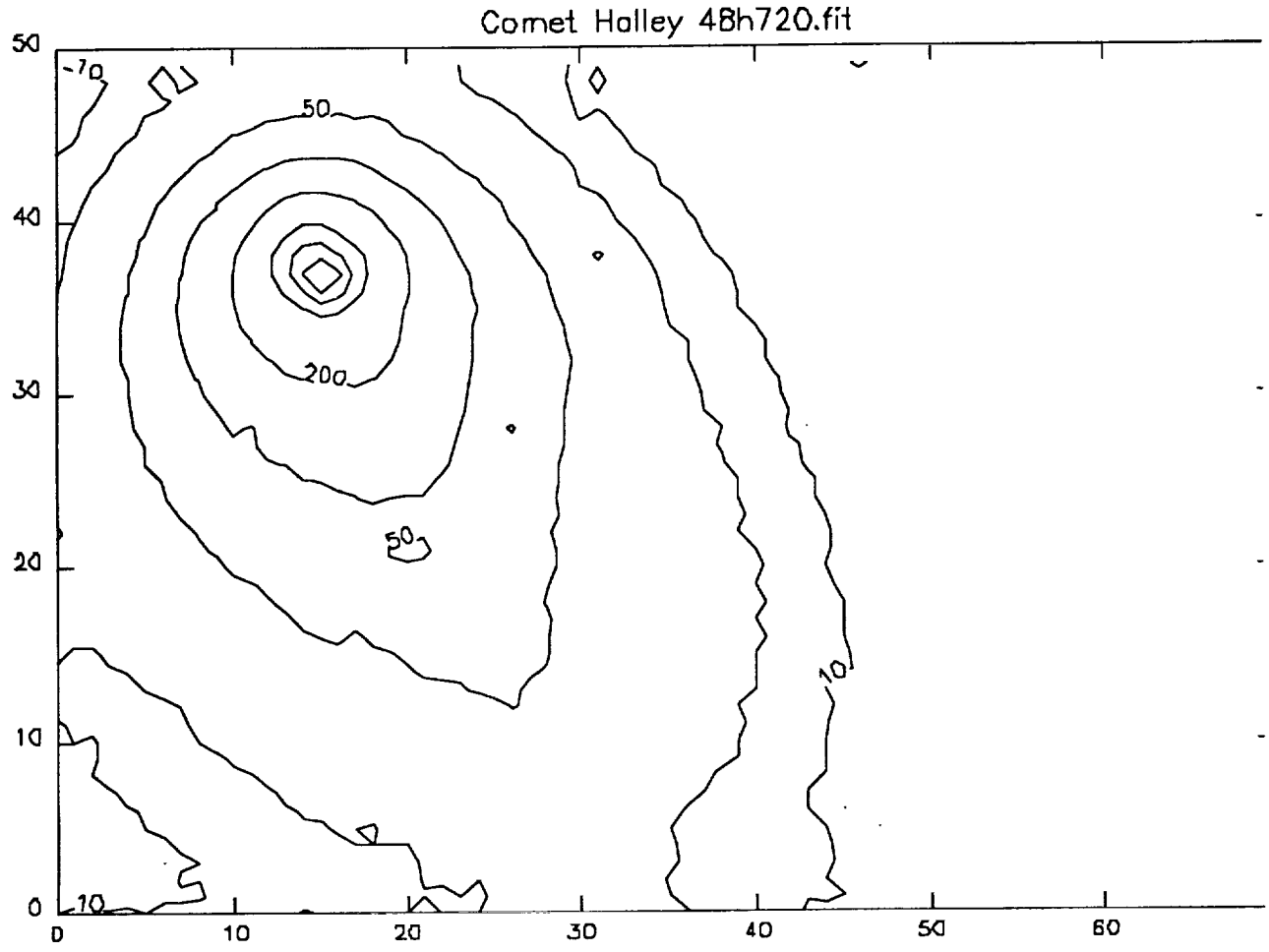

Figure 3. Image of Comet P/Halley at 4840 Å. Shown in a contour plot of an image of comet P/Halley taken with the 61-inch Wyeth telescope at Oak Ridge Observatory on December 30, 1985. The image has been flat-field corrected and background subtracted.

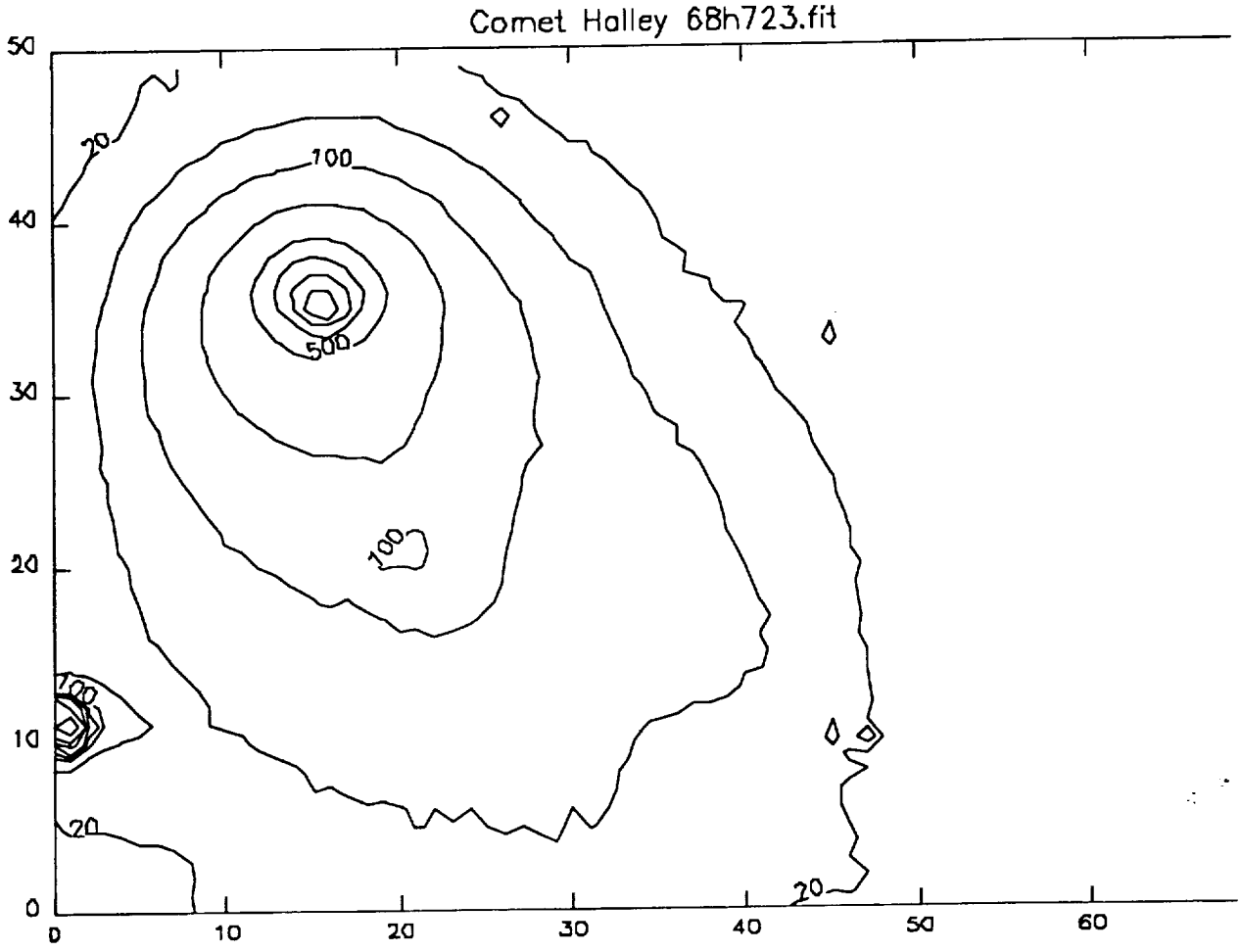

Figure 4. Image of Comet P/Halley at 6840 Å. Shown is a contour plot of an image of Comet P/Halley taken with the 61-inch Wyeth telescope at Oak Ridge Observatory on December 30, 1985. The image has been flat-field corrected and background subtracted.

An interesting and important set of data has become available relating to the distribution of dust in comet P/Halley. As part of the ongoing collaboration with Dr. Uwe Fink of the University of Arizona, we have analyzed spatial profiles (generally sunward and antisunward) of the gas species C_2, CN, NH_2 and $O(^1D)$ in Comet Halley with a time-dependent model which accounts for the 7.4-day periodic variation of the gas production rates (Schleicher et al. 1990). The involvement of this PI for the gas coma work is funded under a separate grant (NAGW-1907). In addition to the gas species data there exists the corresponding spatial profiles of the dust continuum which were actually generated in the process of production of the gas species profiles, since the dust

continuum must be subtracted in order to obtain gas species profiles. The interesting aspect of these data are that sets of adjacent-day observations were made several times during the 1985-1986 apparition of the comet: December 8 and 9, January 10, 11, and 12, March 1 and 2, and April 14 and 15. The most interesting set is that in April where the Schleicher et al. 'light curve' was continuously observed with excellent time coverage.

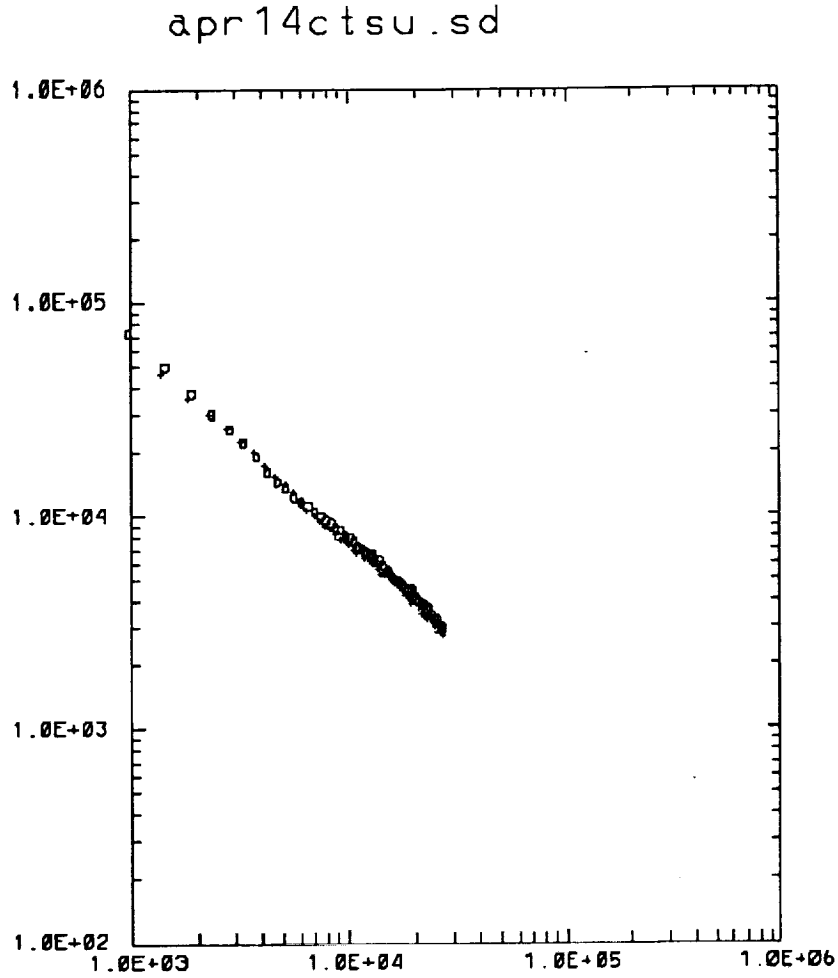

Figure 5. Spatial Profile of Dust Continuum at 6520 Å on April 14.3, 1986. The sunward (+'s) and antisunward (o's) spatial profiles of dust continuum in Comet P/Halley as derived from long-slit spectra taken with the 61-inch telescope at Mt. Lemmon on April 14.3, 1986. The spectrum was recorded on the downward part of the gas production variation (Schleicher et al., 1990) the signature of the high production rate is seen at the outer part produced roughly from one-half to one day before the observation time can be easily seen as the 'bump' outside about 10,000km.

On April 14.3 the comet was on the downward part of the production rate variation whereas by April 15.3 it had passed the minimum and was on the upward part of the curve. Comparison of the sunward and antisunward spatial profiles as shown in Figures 5

and 6 clearly shows evidence of just this type of variation. The portion of the April 14.3 profile outside of 10,000 km clearly shows the effect of the raised production rate at the previous maximum which occurred from one-half to one and one-half days previous to the observation. The April 15.3 profile on the other hand clearly shows the turning-on of the sunward ejecting dust, and also shows that the 'bump' seen on April 14.3 has moved out past the end.

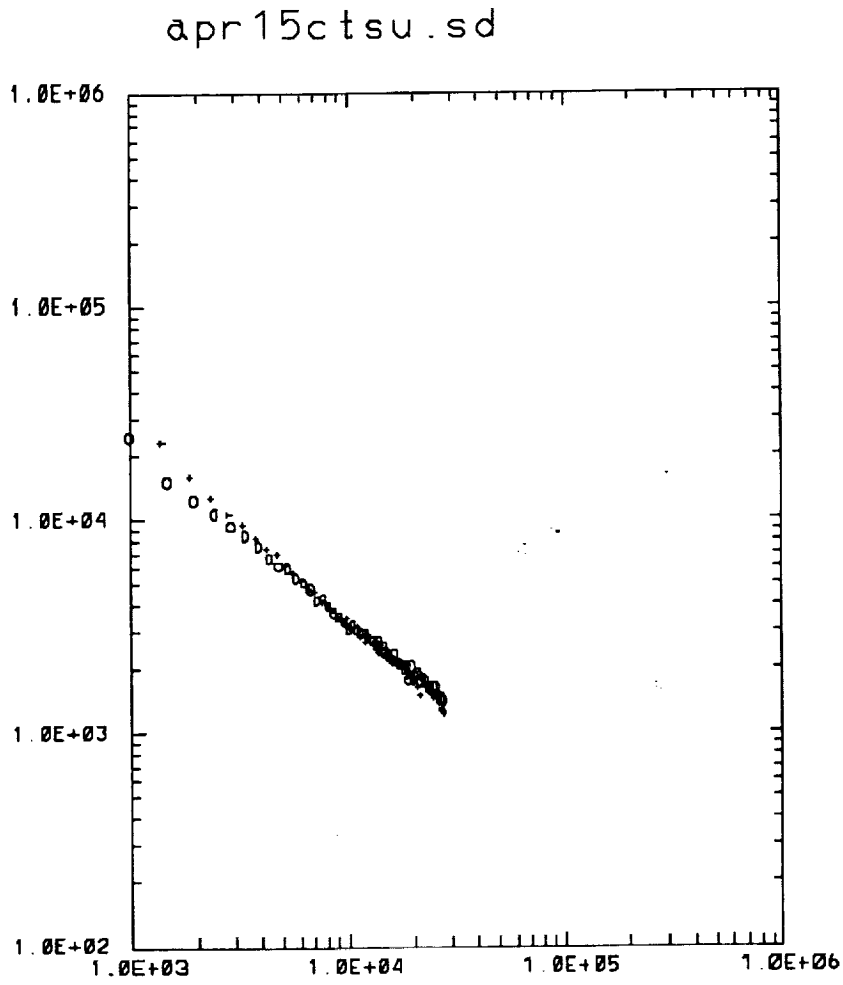

Figure 6. Spatial Profile of Dust Continuum at 6520 Å on April 15.3, 1986. The sunward (+'s) and antisunward (o's) spatial profiles of dust continuum in Comet P/Halley as derived from long-slit spectra taken with the 61-inch telescope at Mt. Lemmon on April 15.3, 1986. The spectrum was recorded on the upward part of the gas production variation (Schleicher et al., 1990) so the high production rate seen at the outer part of the April 14.3 profile seen in Figure 3 has since moved out of the inner coma. The turning-on of the next active region can be seen in the inner part of the sunward profile.

The use of a time-dependent model for the dust production based on the knowledge of the gas production source in combination with the observed profiles helps separate out the effects of production rate variations from dust particle decay and provide hard evidence for the correctness of the variation of dust particle initial (so-called terminal) velocities. In the next section is a discussion of the analysis of the March 1.5 and 2.5 spatial profiles. Analysis of the April 14/15 set will proceed during the next grant year.

IV. Time-Dependent Aspherical Modeling of Halley's Dust Coma

This portion of the project involves the analysis of spatial profiles of the dust continuum which were generated in the process of construction of the gas species profiles of the gas species C_2, CN, NH_2 and $O(^1D)$ in Comet Halley (Fink, Combi and DiSanti, 1991). Explicit time-dependence has been incorporated into the dust model as a parametrized version of the 7.4-day periodic variation of the gas production rates (Schleicher et al. 1990). The interesting aspect of these data are that sets of adjacent-day observations were made several times during the 1985-1986 apparition of the comet: December 8 and 9, January 10, 11, and 12, March 1 and 2, and April 14 and 15.

On March 1 the comet was on the downward part of the production rate variation whereas by March 2 it had passed the minimum and was on the upward part of the curve. At the top of Figure 7a the observed sunward and antisunward profiles have been averaged to approximately "average-out" the effects of day/night asymmetry and radiation pressure. Below this is the result of the model with the 7.4-day period variations corresponding to the same phase lag we found for the gas species (Combi and Fink 1993). It is clear that dust terminal velocities for the important "optical size range" obtained from standard dusty-gas drag calculations provides approximately the correct propagation speed for the varying production rate signal.

In Figures 7b and 7c the actual sunward and antisunward profiles are shown and compared with models where a day/night dust production asymmetry has been included. For this calculation the asymmetry was incorporated as separate weightings for the dayside and nightside hemispheres. What is interesting is that a larger asymmetry (4:1) is required for the March 2 profile which is produced primarily near the peak of the variation as opposed to the March 1 profile (1.2:1) which is produced closer to the minimum. It is clear from this result that the dust emission is a complex function of both time and spatial vector direction since the day/night asymmetry clearly varies with time, and that a substantial nightside ejection is also required in agreement with the close-up Giotto images (Keller et al. 1986). It should also be mentioned here that these are

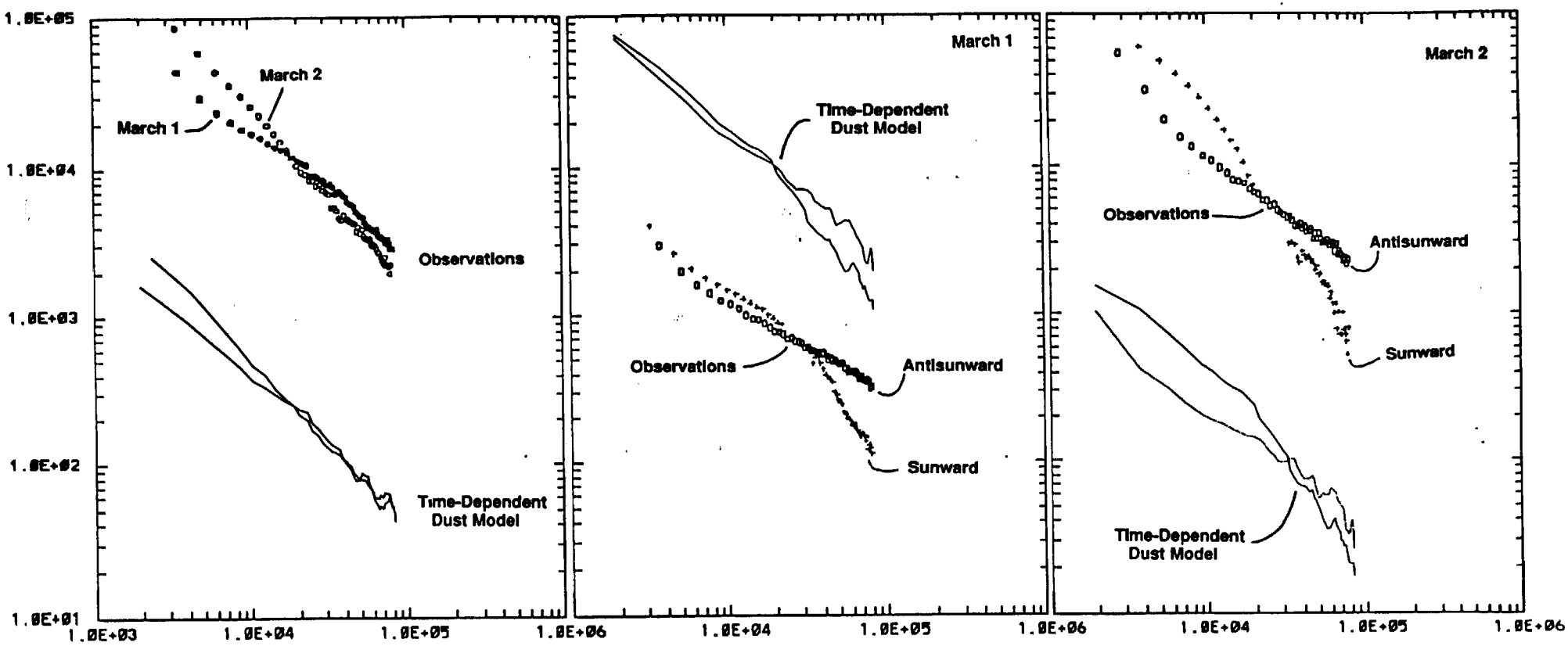

Figure 7. Preliminary Results of the New Cometary Dust Model. All three log-log plots have a relative brightness scale on the vertical axis and the projected distance to the nucleus in km on the horizontal axis. In all cases the observational data are continuum scans at 6520 Å and were obtained from the same long-slit dataset as various molecular spatial profiles published by Fink, Combi and DiSanti (1991). At the left in (a) is shown the average of the sunward and antisunward profiles from data obtained on March 1 and March 2, 1986. The observed profiles have been shifted vertically to account for the relative calibration of the two. The time-dependent dust model accounts for a typical Halley dust size/velocity distribution as well as for the 7.4-day periodic variation in the production rate. The typical velocity distribution does account for the time evolution of the spatial profile using the same 14 hour phase lag as found for the gas species by Combi and Fink (1991). The plots in (b) and (c) show the separate sunward and antisunward profiles compared with models which include day/night asymmetry. The March 1 profiles are fitted with a model where the day/night asymmetry of the initial dust ejection is in the ratio of 0.55 to 0.45. The March 2 profiles on the other hand, require a model with a day/night asymmetry of 0.80/0.20. The March 2 observation was taken when the comet was on the rising part of the light curve implying that the extent of the day/night asymmetry for Halley in fact varied with rotation of the nucleus and that the asymmetry becomes larger as the activity becomes greater.

preliminary results and that neither the dust size distribution nor the optical properties (e.g. Q_{scat}) have been optimized to "fit" the sunward/antisunward radiation pressure asymmetry. It is clear that the radiation pressure distortion is larger in the data and the slope steeper (possible fragmentation?) than the model, although the qualitative agreement is good.

Figure 8a shows the 2-D modeled images of the 6840 Å coma corresponding to the spatial profiles discussed above. The results discussed in this section have been presented at the 1992 Division for Planetary Sciences Meeting in Munich, Germany (Combi and Fink 1992).

V. Modeling Images of the Coma in Two Dimensions

The other (actually the main) part of this study is to try to understand the observed 2-D morphology of the dust coma as seen in filtered CCD images of comets (in particular comet Halley) in terms of the detailed physics of dust particles and their ejection from the inner fluid coma of the comet. Although the reproduction of 1-D spatial profiles is encouraging in terms of the average value of the dust terminal velocities and their average radiation pressure acceleration, the true test comes when trying to reproduce full 2-D images. Keller and co-workers (e.g. see Keller and Meier 1976) demonstrated the importance of analyzing 2-D images of the hydrogen Lyman-alpha coma in a series of papers published over a number of years. Hydrogen atoms, like dust particles, are subject to a strong antisunwardly directed radiation pressure acceleration. The work of Keller showed that the speed distribution of H atoms leaving the inner coma was of the utmost importance in producing the observed shapes of the isophotes in the outer coma.

The principle goes back to a number of old papers beginning with Eddington's (1910) original fountain model, and culminated with the papers by Wallace and Miller (1958) and Haser (1966). For a point source of particles ejected at a single speed and subjected to a single antisunwardly directed acceleration, the "coma" which results appears to have circular isophotes which terminate discontinuously at the projected boundary of the paraboloid of rotation whose vertex is located at a distance of $v^2/2b$ where v is the outflow speed and b is the acceleration. The brightness (which is proportional to the column density) of the circular isophotes is independent of the viewers angle with respect to the sun-comet line, although the projected shape of the paraboloid certainly is.

Keller's work showed that the effective velocity distribution of H atoms in a bright comet like Kohoutek had to be composed of a broad distribution of speeds ranging from 1-2 km/s up to speeds exceeding 20 km/s. It was the later papers by Combi and Smyth

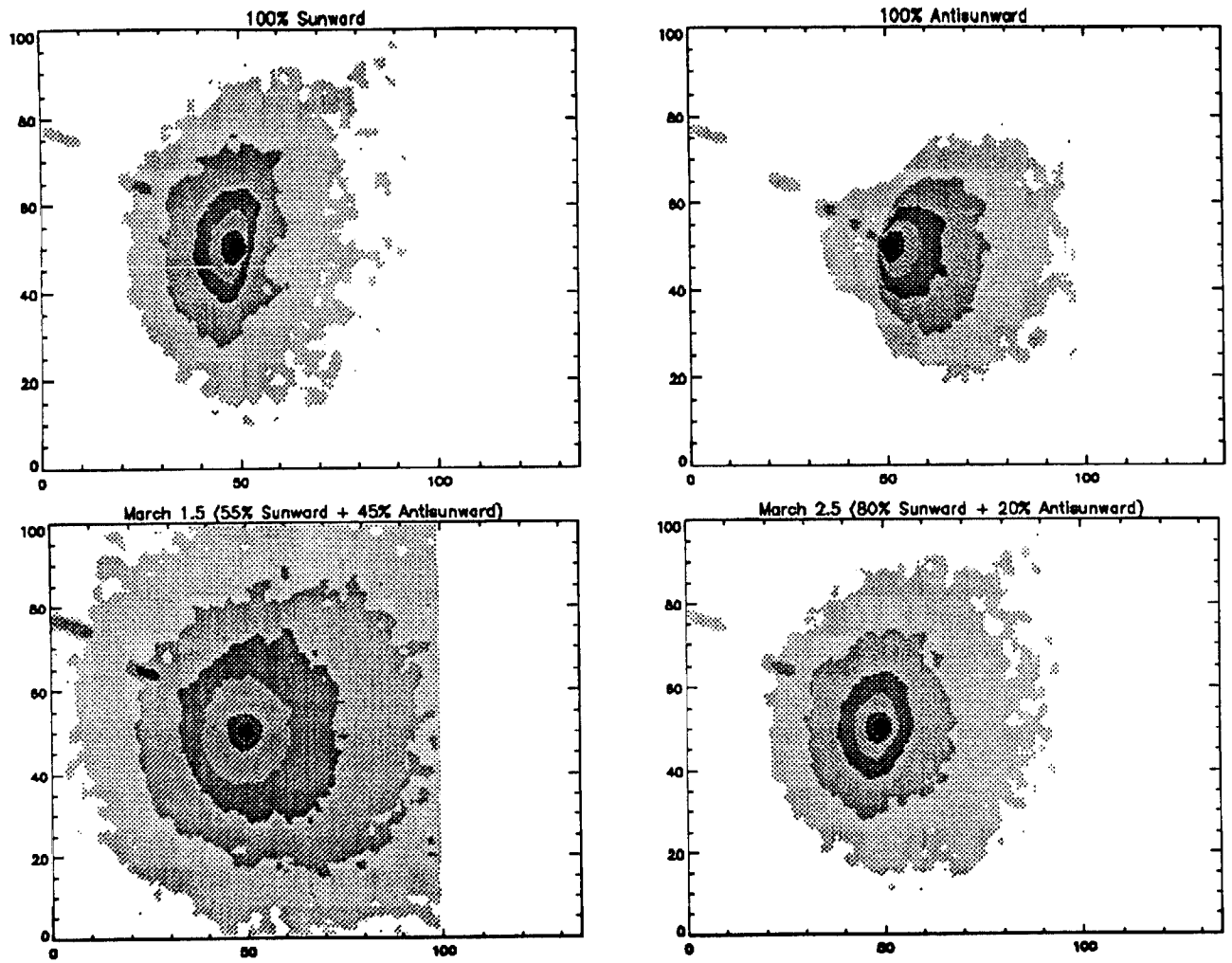

Figure 8. Modeled Two-Dimensional Images of the Dust Coma of Halley's Comet. The two upper images correspond to 100% sunward and 100% antisunward emission for the March 1-2, 1986, epoch. Below are the two images which correspond to the best-fit combinations of weighted sunward-antisunward emission that reproduce the spatial profiles determined from the long-slit spectra on March 1.5 to the left and March 2.5 to the right. See text for details.

(1988b) and Smyth, Combi and Stewart (1991) which showed that a velocity distribution similar to but much more irregular than the 3 Maxwellians in Keller and Meier (1976) is a natural by-product of water and OH photodissociation in combination with partial collisional thermalization of H atoms before they exit the inner coma.

Figures 2 and 3 are quite representative of isophote maps of the dust comae of many comets which have been reproduced from photographic plates. Curiously, the isophotes almost always look rather elongated, being more reminiscent of the H Lyman-alpha isophotes and not as much like more circular ones which the dust models produces. This is because of the one-to-one-to relationship between the dust particle size, terminal velocity and radiation pressure acceleration. Although in our formulation this relationship is complicated by the variable dust density and the non-linear relationship from the gasdynamic drag, it is still the case that for the range of sizes of dust particles which dominate the in the visual images that the value of $v^2/2b$ is only a weakly variable quantity. This is analogous to the fact that the critical parameter in the standard Finson-Probstein method is not the particle size but the parameter (ρd), the product of the density and diameter. The cross section of a dust particle increases as the square of the radius (or diameter) whereas its mass increases as the cube. Both the terminal velocity (owing to gas drag) and the radiation pressure acceleration are larger for smaller particles, therefore the shapes of the isophote distributions over a fairly wide range of particle sizes do not vary very much.

In order to produce the elongated isophotes such as are seen in the H coma one requires a range of effective radial outflow speeds but a single value for the radiation pressure acceleration. However, it is clear from our "more physically realistic" dust models that we do not get elongated isophotes. Like the H atom coma we require a wide range of terminal velocities for particles of a certain size rather than just the one-to-one-to-one relationship between particle size, particle velocity and particle radiation pressure acceleration.

A reasonable solution to this is that as dust particles are accelerated by gasdynamic drag in the inner 100-300 km of the coma that dust particle fragmentation is a dominant process. As particles fragment they produce many smaller pieces, however the gas-drag acceleration is the largest only very close to the nucleus. Therefore small particles produced by fragmentation of larger particles farther from the nucleus will be traveling at smaller velocities than small particles produced near the nucleus where the gas-drag is large.

Particle fragmentation is certainly not a new idea. It has been suggested as a mechanism to explain radial profiles which vary more steeply than the 1/r expected for a

point source. It has also been suggested more recently as a possible explanation for the radial profiles extracted from the Giotto images of the very inner coma comet Halley. Where the arguments here differ is that we contend that particle fragmentation in the acceleration region is a common property of all comets which are moderately productive.

It is reasonable to speculate that cometary dust particles themselves are very fragile and that the gasdynamic drag in addition to accelerating the particles also fragments them. This fragmentation would occur only in the very innermost coma. If the fragmentation simply breaks up large particles into smaller ones then the process will increase the effect surface area per unit mass, explaining the flattened dust profiles in the Giotto images. Since we can calculated the forces on dust particles from the gas drag then this sets an order of magnitude as to the bulk strength of the aggregates of cometary dust.

The modeling difficulty presented by this result means that the dust particle size distributions inferred by Finson-Probstein analysis may be totally wrong because the one-to-one-to-one relationship between size, velocity and acceleration no longer holds. Also the dust particle size distribution itself seen at some distance from the nucleus is a by-product of the acceleration/fragmentation by gasdynamic drag in the first few tens of km from the nucleus.

To test our hypothesis of dust fragmentation we have run a heuristic dust size-velocity distribution. We start with the normal Hanner type distribution we used above to describe the original dust particle distribution and calculate its terminal velocity from the Sekanina approximation. Then we redistribute each particle over all possible fragment sizes. In the realm of Monte Carlo we simply choose some particle size smaller than the original size for the purpose of calculating the radiation pressure acceleration. A reasonable and simple choice for the redistribution function is as follows. If "a_o" is the original particle size (for the purpose of calculating the terminal velocity) the fragmented size is calculated from

$$a = a_o R_i^p$$

where Ri = a random number on the interval from 0 to 1, and

p = an adjustable parameter.

In the absence of a fundamental model for the original dust-size distribution and the dust fragmentation process this form has an adjustable parameter, p, which describes in some reasonable way the redistribution by the fragmentation of original large particles.

The choice of Hanner-type distribution is in some sense ad hoc especially when combined with this heuristic redistribution function.

Figure 9a shows a contour plot of an image of comet Halley obtained at the Oak Ridge Observatory by R.E. McCrosky. Figures 9 b and c show two models for the original Hanner-type distribution which yields the more circular isophotes as well as that obtained using the fragmentation/redistribution model with the parameter p taken to be 1.5. This value yields a reasonable match to the overall radiation pressure distortion as well as to the shapes of the elongated isophotes.

Although this is far from a unique solution it nonetheless demonstrates that there clearly cannot be a one-to-one-to-one relationship between particle size, velocity and radiation pressure acceleration. Furthermore, the production of slower small particles by fragmentation of originally larger particles make sense physically and is a reasonable solution to the distribution of dust in the innermost coma of comet Halley as seen in the Giotto images. Therefore, although the details of the size-velocity relation in the heuristic model shown here is probably not exactly correct it does contain the essential elements of the correct distribution, i.e. a distribution of particle velocities for each particle size. Specifically, the elongated shapes of dust coma isophotes require the existence of a substantial population of small but slow particles which must be produced by the fragmentation of initially larger particles.

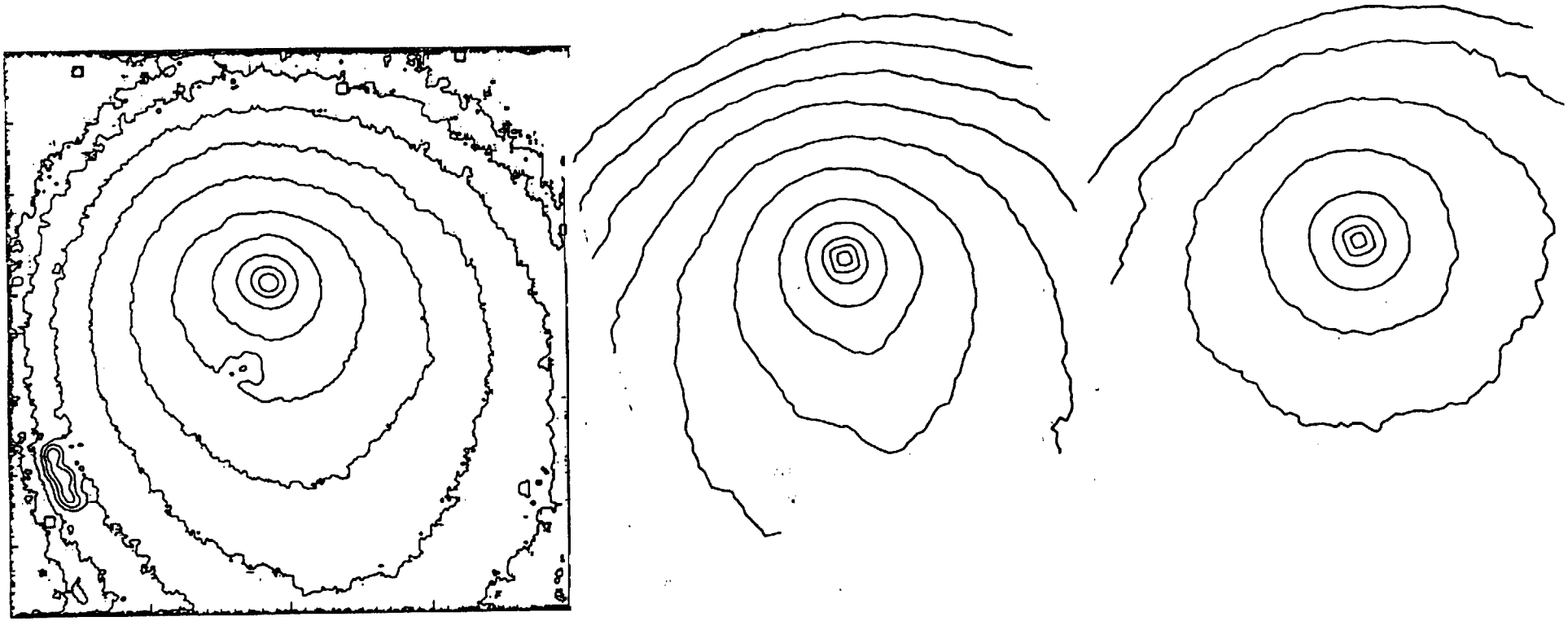

Figure 7. Comparison of Fragmentation Model with Data . To the left is a contour plot of a 6840 Å image of comet Halley recorded on Dec 3.82, 1985, with the 61-inch Wyeth telescope at the Oak Ridge Observatory by Dr. R.E. McCrosky. The sunward direction is toward the upper left (at about 10 o'clock). Contours are at intervals of a factor of two. To the right is a model contour plot corresponding to the same image from the "standard model" using the Hanner-type particle size distribution and the one-to-one-to-one correspondence of particle size to terminal velocity to radiation pressure acceleration. Clearly the overall map looks not much different from the Wallace and Miller point source which produced circular isophotes within a paraboloid. In the middle is the heuristic fragmentation model where particles are redistributed according to the power law discussed in the text with the parameter p taken to be 1.5. For values larger than 1.5 (2 for example) the isophotes are much more elongated than the data, whereas for values less than 1.5 the isophotes are too circular. The power-law mimics the kind of spread in particle size one might expect from particle fragmentation within the acceleration region. The edge of the square image corresponds to about 140,000 km at the comet.

VII. References

Combi, M.R. The Outflow Speed of the Coma of Halley's Comet. *Icarus* **81**, 41, 1989.

Combi, M.R. and W.H. Smyth. Monte Carlo Particle Trajectory Models for Neutral Cometary Gases. I. Models and Equations. *Astrophys. J.* **327**, 1026, 1988.

Combi, M.R. and W.H. Smyth. Monte Carlo Particle Trajectory Models for Neutral Cometary Gases. II. The Spatial Morphology of the Lyman-alpha Coma. *Astrophys. J.* **327**, 1044, 1988.

Combi, M.R. and U. Fink. Time-Dependent Aspherical Modeling of the Spatial Profiles of Dust in Comet Halley. *Bull. A. A. S.* **24**, 1018, 1992.

Combi, M.R. and U. Fink. P/Halley: Effects of Time-Dependent Production Rates on Spatial Emission Profiles. *Astrophys. J.* (In press), 1993.

Eddington, A.S. The Envelopes of Comet Morehouse (1908c). *Mon. Not. Roy. Astron. Soc.* **70**, 442-458, 1910.

Ellis, T.A. and J.S. Neff. Numerical Simulation of the Emission and Motion of Neutral and Charged Dust from P/Halley. *Icarus* **91**, 280-296, 1991.

Fink, U. , M.R. Combi and M.A. DiSanti. P/Halley: Spatial Distributions and Scale Lengths for C_2, CN, NH_2 and H_2O. *Astrophys. J.* **383** ,356-371, 1991.

Finson, M.L. and R.F. Probstein. A Theory of Dust Comets. I. Model and Equations. *Astrophys. J.* **154**, 327-352, 1968a

Finson, M.L. and R.F. Probstein. A Theory of Dust Comets. II. Results for Comet Arend-Roland. *Astrophys. J.* **154**, 353-380, 1968b.

Gombosi, T.I. A Heuristic Model of the Comet Halley Dust Size Distribution. In *20th ESLAB Symposium on the Exploration of Halley's Comet*, Eds. B. Basttrick, E.J. Rolfe, R. Reinhard, ESA SP-250 II p 167-171.

Gombosi, T.I., T.E. Cravens, and A.F. Nagy. Time-dependent Dusty Gas Dynamical Flow Near Cometary Nuclei. *Astrophys. J.* **293**, 328-341, 1985.

Gombosi, T.I., A.F. Nagy, and T.E. Cravens. Dust and Neutral Gas Modeling of the Inner Atmospheres of Comets. *Rev. Geophys.* **24**, 667-700, 1986.

Haser, L. Calcul de Distribution d'Intensité Relative dans une Tet Cométaire. *Mem. Soc. Roy. Soc. Liege*, Ser. 5, **12**, 233-241, 1966.

Hellimich, R. and G.H. Schwehm. Prediction of Dust Particle Number Flux and Fluence Rates for the EDA-Giotto and USSR Vega Missions to Comet Halley: A Comparison. In *Cometary Exploration*, Ed. T.I. Gombosi,. Central Research Institute for Physics, Hungarian Academy of Sciences; Budapest, III, p. 175-183.

Hoban, Susan, Michael F. A'Hearn, Peter V. Birch and Ralph Martin. Spatial Structure in the Color of the Dust Coma of Comet P/Halley. *Icarus* **79**, 145-158, 1989.

Huebner, W.F., D. C. Boice, H. Reitsema, W.A. Delamere, and F.L. Whipple. A Model for the Intensity Profiles of Dust Jets Near the Nucleus of Comet Halley. *Icarus* **76**, 78-88/

Jewitt, David and Jane Luu. A CCD Portrait of Comet P/Tempel 2. *Astron. J.* **97**, 1766-1790, 1990.

Keller, H.U. and R.R. Meier. A Cometary Hydrogen Model for Arbitrary Observational Geometry. *Astron. Astrophys.* **23**, 269-280, 1976.

Keller, H.U., et al. Comet Halley's Nucleus and Its Activity. Astron. Astrophys. **187**, 807-823, 1987.

Lamy, P. L., E. Grün and J.M. Perrin. Comet P/Halley: Implications of the Mass Distribution Function for the Photopolarimetric Properties of the Dust Coma. *Astron. Astrophys.* **187**, 767-773, 1987.

Marconi, M.L. and D.A. Mendis. The Atmosphere of a Dirty-clathrate Cometary Nucleus: A Two-Phase, Multi-Fluid Model. *Astrophys. J.* **273**, 381-396, 1983.

Mukai, S., T. Mukai and S. Kikuchi. Observations of comet P/Halley at Minimum Phase Angle. *Astron. Astrophys.* **187**, 650-652, 1987.

Schleicher, D.G. et al. Periodic Variations in the Activity of Comet P/Halley during the 1985/1986 Apparition. *Astron. J.* **100**, 896-912, 1990.

Smyth, W.H., M.R. Combi and A.I.F. Stewart. Analysis of the Pioneer-Venus Lyman-1 Image of the Hydrogen Coma of Comet P/Halley. *Science* **253**, 1008-1010, 1991.

Probstein, R.F. The Dusty Gas Dynamics of Comet Heads. In *Problems of Hydrodynamics and Continuum Mechanics*, p 568, Society for Industrial and Applied Mathematics, Philadelphia,Pa., 1968.

Sekanina, Z. Distribution and Activity of Discrete Emission Areas on the Nucleus of Periodic Comet Swift-Tuttle. *Astron. J.* **86**, 1741-1773, 1981.

Sekanina, Z. and S.M. Larson. Coma Morphology and Dust-Emission Pattern of Periodic Comet Halley. II. Nucleus Spin Vector and Modeling of Major Dust Features in 1910. *Astron. J.* **89**, 1408-1418, 1984.

Wallace, L.V. and F.D. Miller. Isophote Configurations for Model Comets. *Astron.J.* **63**, 213-219, 1958.

Wallis, M.K. Dusty Gasdynamics in Real Comets. In *Comets*, Ed. L.L Wilkening, University of Arizona Press; Tucson, AZ, p. 357-369.

APPENDIX

"Time-Dependent Aspherical Modeling of the Spatial Profiles of Dust in Comet Halley"

by M.R. Combi and U. Fink

Division for Planetary Sciences Meeting, Munich, Germany, October 1992
Bull. A. A. S. **24**, 1018.

Time-Dependent Aspherical Modeling of the Spatial Profiles of Dust in Comet Halley

Michael Combi (AOSS/SPRL, U.Michigan)
and
Uwe Fink (LPL, U. Arizona)

Contributions by Michael DiSanti (GSFC)
Al Schultz (ST Sci. Inst.)

Observations

- Long-slit CCD spectra taken throughout the Halley apparition
- 164 cm Catalina Site Telescope of the University of Arizona
- 180 x 800 of an 800 x 800 Tl CCD: 205" x 5200 Å - 10400 Å
- Spatial profiles C2, CN, NH2, O(1D), and continuum
  Fink, Combi and DiSanti (1991, ApJ 383,356)
  Fink and DiSanti (1990, ApJ 364,687)
  DiSanti, Fink and Schultz (1990, Icarus 86,152)

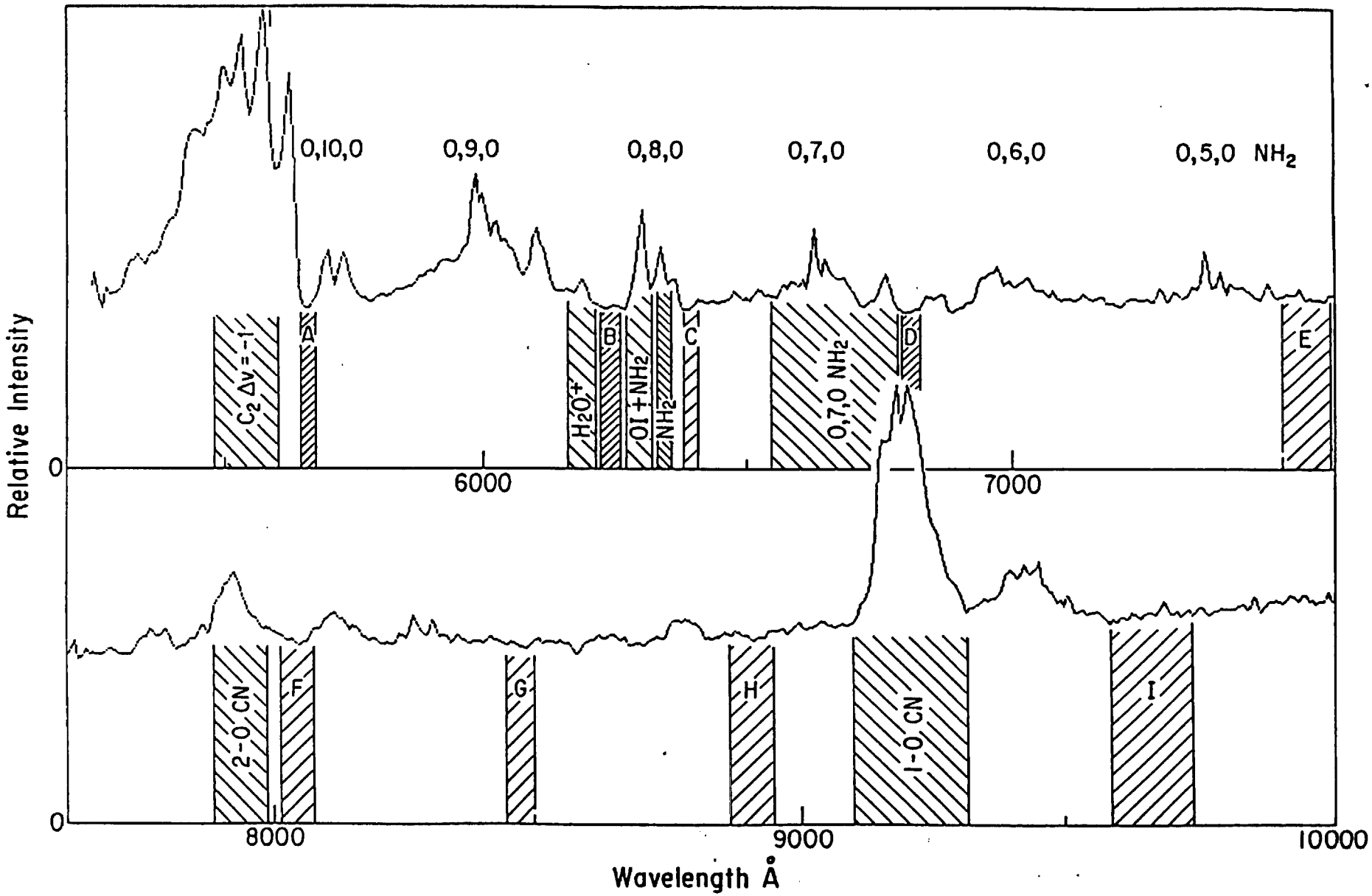

Fig. 1 Ratio spectrum of comet P/Halley on 1986 Jan. 11, showing the placement of our emission windows for C_2, H_2O^+, OI, NH_2 0,8,0 and 0,7,0, and CN 2-0 and 1-0 bands as well as our continuum windows (labelled by letters *A-I*). Continuum strips were determined not only by this exposure but were picked by examining the whole gamut of our P/Halley spectra from 1985 August to 1986 June.

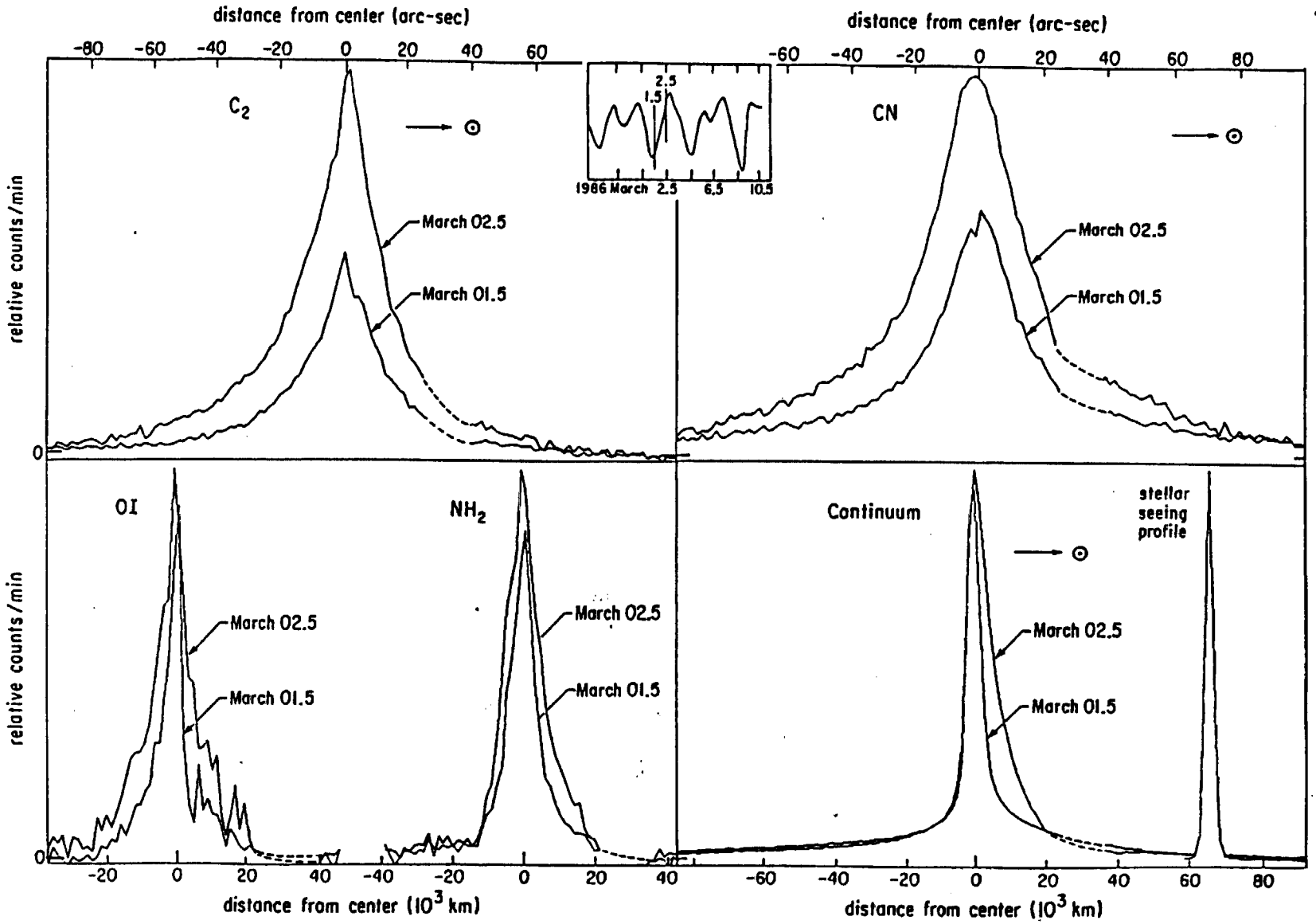

Fig. 6 Comparison of spatial profiles for 1986 March 1.5 near a lightcurve minimum, and March 2.5 near a lightcurve maximum. The inset shows the extrapolated lightcurve of P/Halley (Millis and Schleicher 1986) on which we have indicated our observation dates. The plots for each species are scaled to equal counts/min. All profiles are shown with the correct signal levels at the end of the slit. The slit was aligned along the tail. Sunward direction is to the right. A stellar seeing profile from comparison star BS 6998 is shown at bottom right. The differences in the profiles between March 1.5 and March 2.5 are considerable. Especially noteworthy is the strong asymmetry toward the sun exhibited by the March 2.5 continuum profile and to a somewhat lesser extent by NH_2 and OI.

Dust Coma Model

I. Basic Framework

- Based on the Monte Carlo trajectory code for the H coma
  Combi and Smyth (1988a, ApJ 327, 1026)
  " (1988b, ApJ 327, 1044)
  Smyth, Combi and Stewart (1991, Science 253, 1008)
  Combi and Feldman (1992, Icarus 97, 260)

- Heliocentric particle orbits in 3-D with radiation pressure

- Collects brightness (and density) contributions in a grid projected on the plane of the sky ==> spatial profiles, maps

Dust Coma Model

II. Dust physics: astronomical silicates -- dark porous aggregates

- **Gombosi (1986) size distribution**
- **Lamy et al (1987) dust density: $\rho(a) = 2.2 - 1.4\, a/(a_o - a)$ g cm $^{-3}$**
- **Sekanina and Larson (1984) method for terminal velocities (reasonable approximation to dusty-gasdynamic calculation)**
- **Mukai et al. (1987) for light scattering efficiency**
- **Hellmich and Schwehm (1983) for radiation pressure efficiency**

- **$Q \sim r^{-2.3}$ pre-perihelion (Schleicher, private communication)**
  $\sim r^{-1.9}$ post-perihelion

- **7.37-day periodic variation -- phase lag and amplitude correction to the Schleicher et al (1990) lightcurve from spatial profile analysis of C2, CN, NH2 and O(1D) by Combi and Fink (1992)**

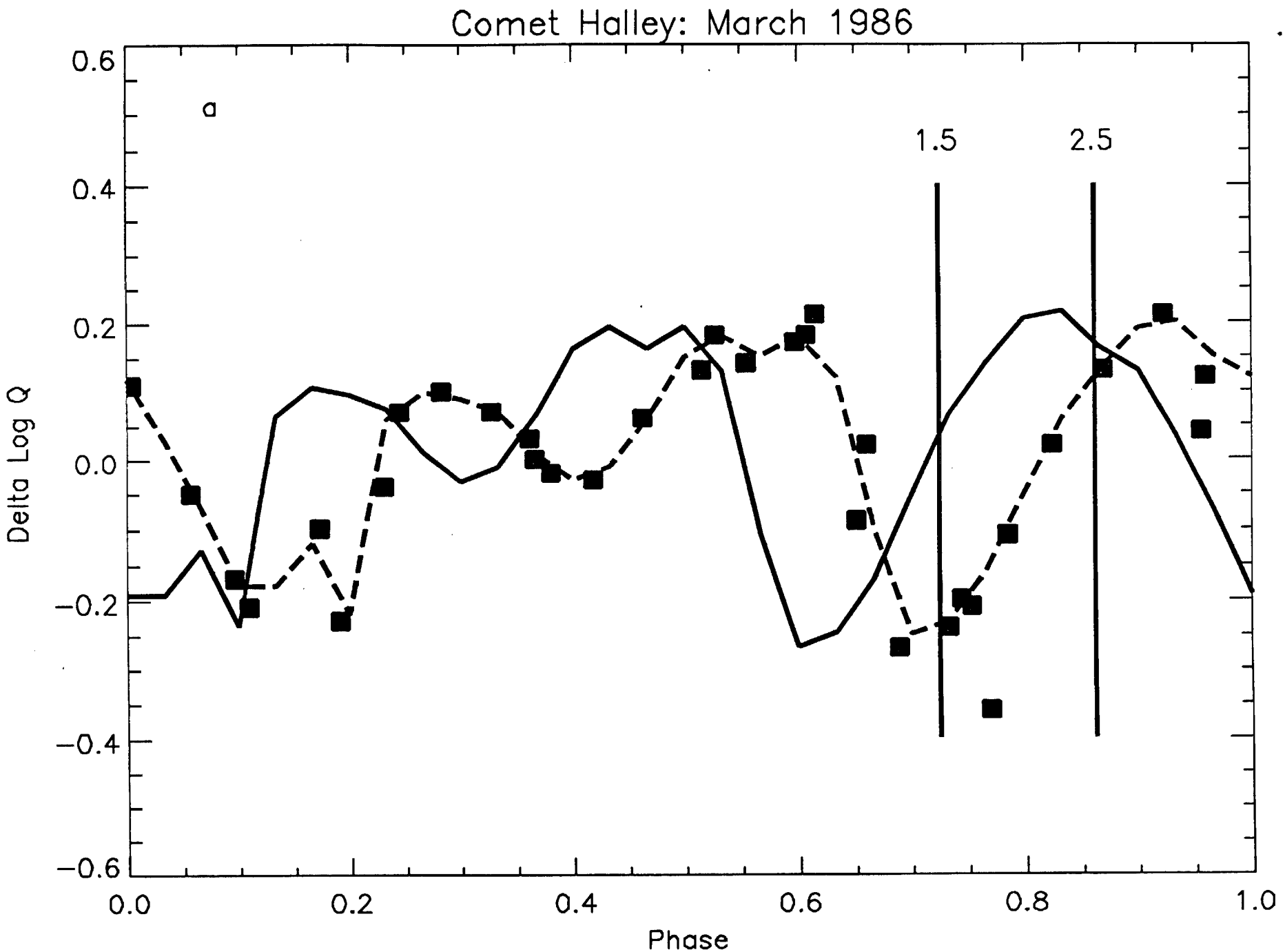
Comet Halley: March 1986
a
1.5
2.5
0.6
0.4
0.2
0.0
−0.2
−0.4
−0.6
Delta Log Q
0.0
0.2
0.4
0.6
0.8
1.0
Phase

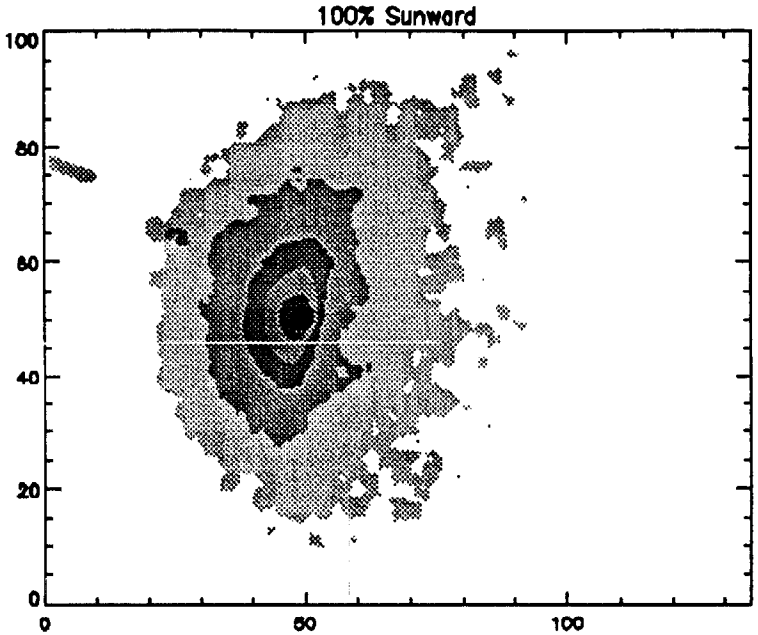
100% Sunward
100
80
60
40
20
0
0
50
100

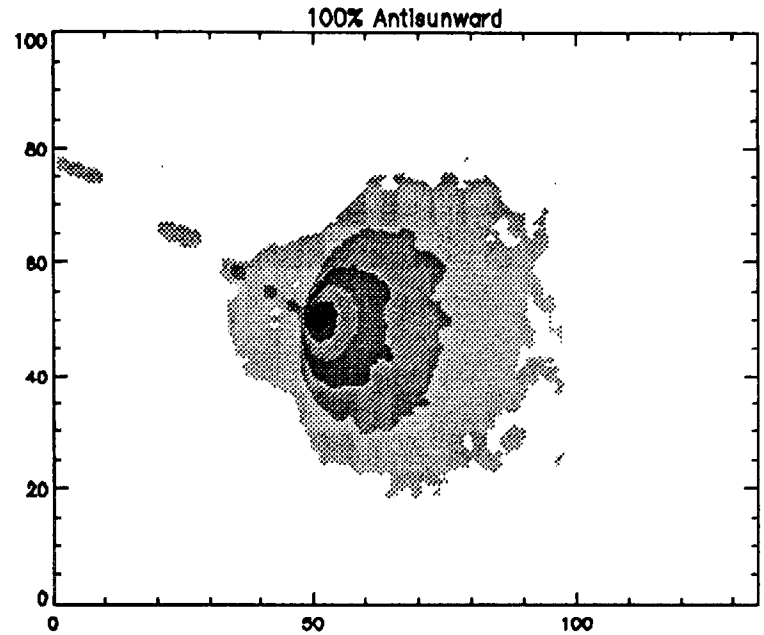
100% Antisunward
100
80
60
40
20
0
0
50
100

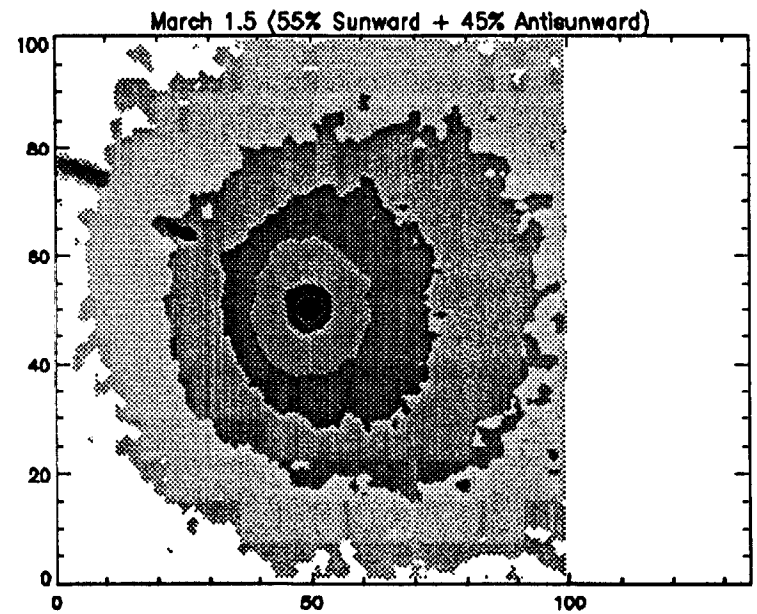
March 1.5 (55% Sunward + 45% Antisunward)
100
80
60
40
20
0
0
50
100

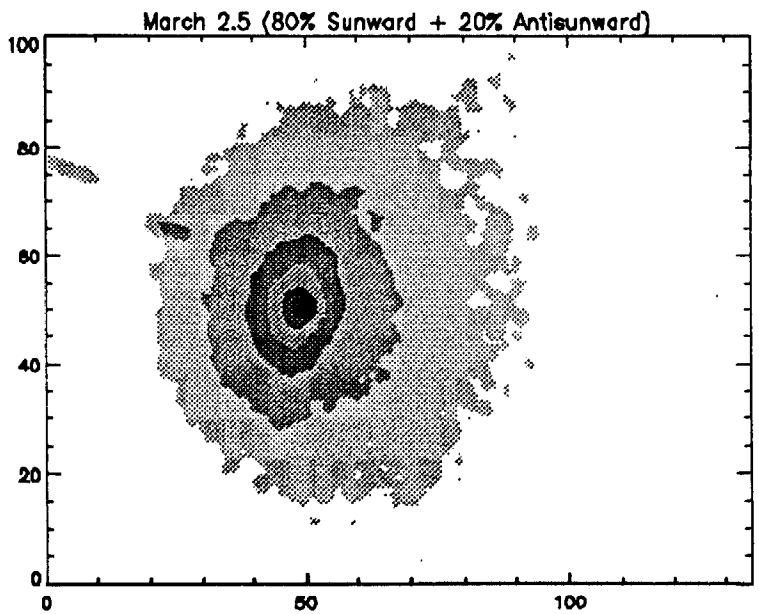
March 2.5 (80% Sunward + 20% Antisunward)
100
80
60
40
20
0
0
50
100

Dust Model Configurations (March 1.5 and 2.5, 1986)

1. **Compare sunward/antisunward averaged profiles**
   - **to test periodic variation amplitude and phase**
   - **radial velocity of dust ~ propagation of "signal"**

2. **Dayside and nightside weighted hemispherical distributions**
   - **to study separate sunward and antisunward profiles**

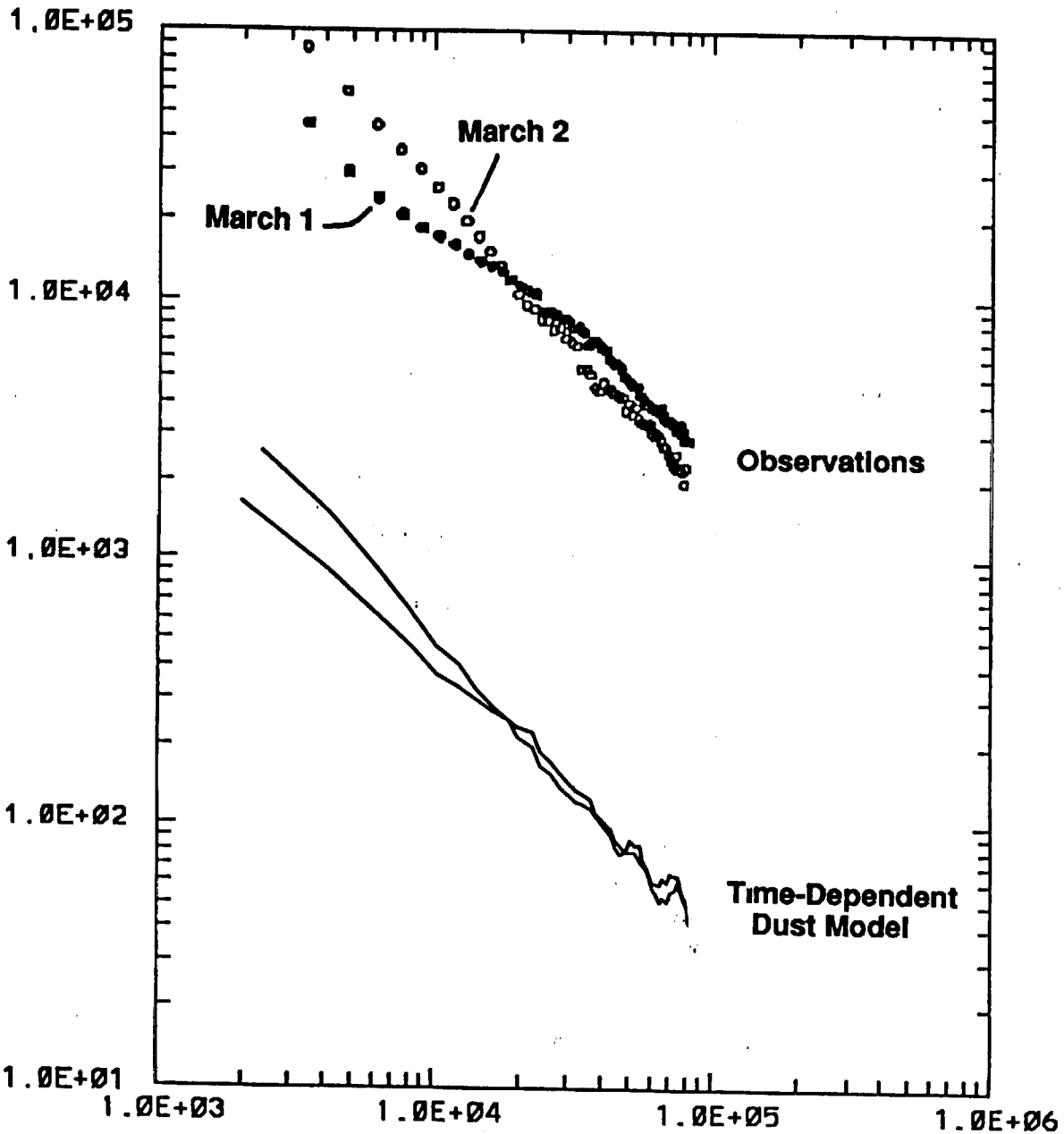
1.0E+05
1.0E+04
1.0E+03
1.0E+02
1.0E+01
1.0E+03
1.0E+04
1.0E+05
1.0E+06
March 2
March 1
Observations
Time-Dependent
Dust Model

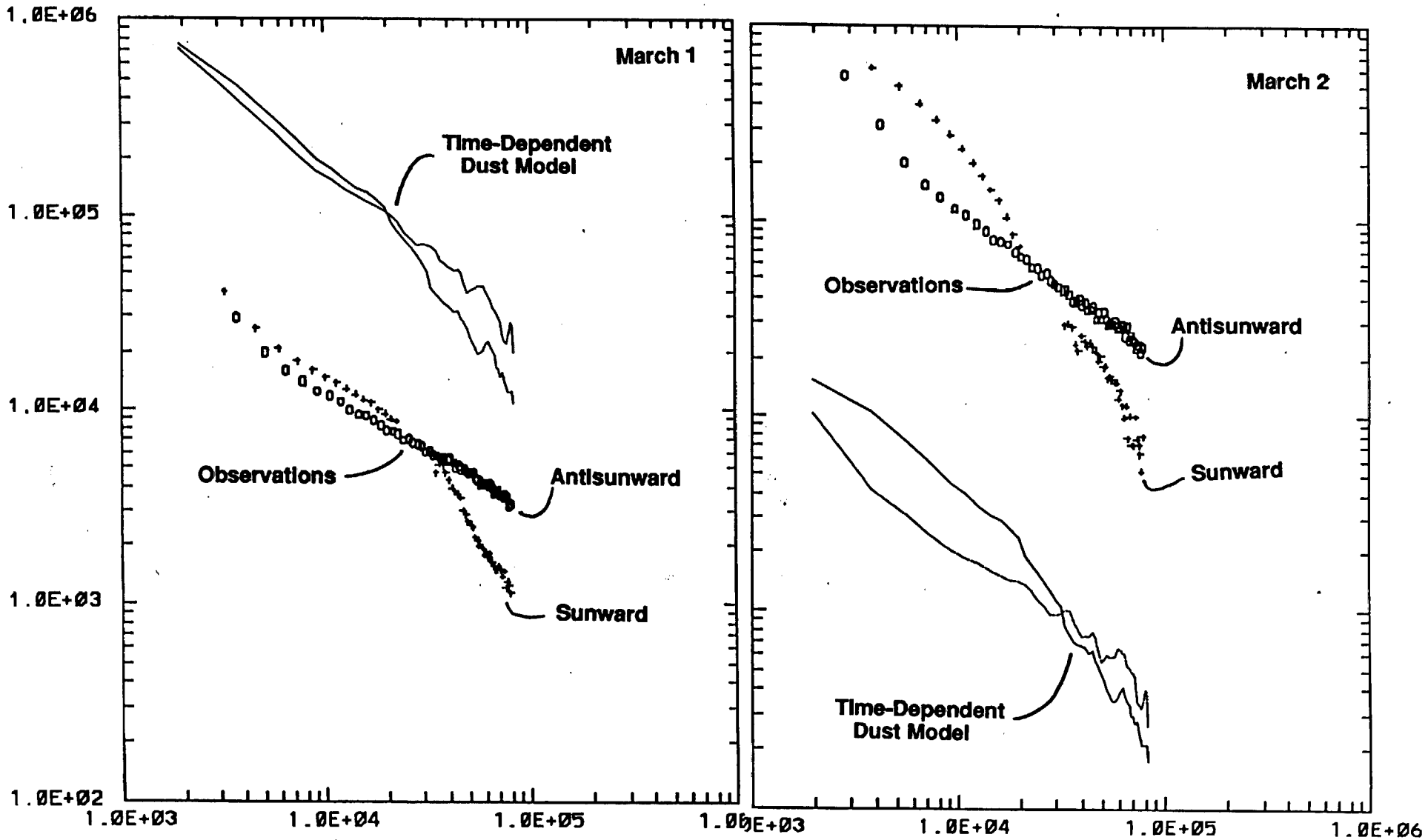
1.0E+06
1.0E+05
1.0E+04
1.0E+03
1.0E+02
1.0E+03
1.0E+04
1.0E+05
1.0E+06
March 1
Time-Dependent
Dust Model
Observations
Antisunward
Sunward
March 2
Observations
Antisunward
Sunward
Time-Dependent
Dust Model

Results

- The same amplitude and phase of the 7.37-day periodic variation production rate explains both gas and dust at the source (although the photometry of separate species and continuum may be somewhat different)

- The asphericity of the comet seems to vary with the level of the periodic variation ==> higher Q ~ larger asymmetry

- Spatial profiles require a significant antisunward ejection of dust

- Possible that the troughs of the 7.37-day variation represent the level of the spherical source and that the higher regions of the lightcurve represent essentially sunward ejected dust